From nanospheres to micelles: simple control of PCL-g-PEG copolymers amphiphilicity through thiol–yne photografting

Assala Al Samad, Youssef Bakkour, Fanny Coumes, Fawaz El Omar, Jean Coudane, Benjamin Nottelet

From nanospheres to micelles: simple control of PCL-*g*-PEG copolymers' amphiphilicity through thiol–yne photografting†

Assala Al Samad,[a,b] Youssef Bakkour,[b] Coumes Fanny,[a] Fawaz El Omar,[b] Jean Coudane[a] and Benjamin Nottelet*[a]

A simple method for the synthesis of a family of poly(ε-caprolactone)-*g*-polyethylene glycol (PCL-*g*-PEG) copolymers of controlled amphiphilicity and their use in generating nanospheres or micelles are reported. PCL-*g*-PEGs with various compositions are prepared from a single strategy relying on a combination of post-polymerization modification and subsequent thiol–yne photografting. Alkyne-functional PCL (PCL-yne) was first obtained by anionic activation and reaction with propargyl bromide to yield PCL-yne with 8% alkyne groups. PEG-thiol is then reacted on PCL-yne under UV activation to yield the targeted graft copolymer by thiol–yne photoaddition. The advantage of the approach is that control over the composition is easily achieved, yielding amphiphilic graft copolymers with ethylene glycol/caprolactone (EG/CL) ratios ranging from 0.1 to 1.3. Starting from this single strategy, it was therefore possible to obtain nanospheres ($D_H \sim 55$ nm) or micelles ($D_H \sim 30$ nm) by copolymer self-assembly depending on the EG/CL ratio. The potential of PCL-*g*-PEG micelles as drug carriers was finally evaluated with curcumin that was efficiently encapsulated, protected and released over 80 days. Interestingly it was found that drug encapsulation efficiency and drug loading were higher for PCL-*g*-PEG copolymers compared to block PCL-*b*-PEG.

Introduction

With almost one-third of newly discovered drugs being highly insoluble in water, the last few decades have witnessed increasing numbers of research studies focused on drug delivery systems able to overcome this solubility limitation.[1] Although various systems exist, including molecular complexation systems based on cyclodextrins, nanosuspensions, lipid formulations, prodrugs, *etc.*,[2] amphiphilic polymeric systems have been widely investigated for their potential applications in pharmaceutical fields. In particular, polymeric micelles and stealth nanospheres have attracted great interest as a result of their unique combination of advantages: drug solubilization and protection, increased circulation times, stability, controlled drug release rate, enhanced therapeutic efficacy, reduced side effects and targeting possibilities.[3–6]

Classical self-assembled polymeric drug carriers involve AB- or ABA-type block copolymers, which spontaneously form nano-sized objects in aqueous medium as a result of the hydrophobic and hydrophilic blocks interacting differently with the solvent. Most studies have focused on linear block copolymers based on poly(ethylene glycol) (PEG) and polyesters like poly(lactide) (PLA), poly(lactide-*co*-glycolide) (PLGA) or poly(ε-caprolactone) (PCL) because of their biocompatibility and biodegradability.[7–11] However, micelles' properties can be advantageously improved by using alternative polymers or architectures. For example, degradation and drug loading can be modulated by using more hydrophobic poly(hexyl-lactide) blocks,[12,13] while micelles' stability can be increased towards serum and lyophilization by using graft structures instead of block copolymers.[14,15] Indeed, graft copolymers are known to have lower critical micellar concentration (CMC) than their linear analogs because of the side chains reducing their mobility and due to their higher polydispersity.[16,17] In addition, graft copolymers have the advantage of allowing an easy variation of the number of PEG chains along the polymer backbone.

Various strategies have therefore been reported to synthesize polyester-*g*-PEG structures, with the two main ones being the "grafting through" and "grafting to" strategies. The "grafting through" strategy is based on the ring opening

[a]*Institute of Biomolecules Max Mousseron (IBMM – CNRS UMR 5247), Department of Artificial Biopolymers – University of Montpellier, France. E-mail: benjamin.nottelet@univ-montp1.fr*
[b]*Laboratory of Applied Chemistry, Doctoral School of Sciences and Technology, Lebanese University, Lebanon*
† Electronic supplementary information (ESI) available.

polymerization of PEG-functional lactones and leads to high grafting density.[18,19] However, in addition to the low yield for lactone synthesis due to multistep reactions, the bulky nature of the monomers can result in polymerizations being slow and limited to low monomer conversions and chain lengths. On the other hand, the "grafting to" strategy allows the polymer backbone and side arms to be separately prepared and characterized prior to their coupling, but at the cost of limited grafting density as a consequence of steric hindrance between the bulky side arms.[20] This strategy has however gained considerable interest in recent years as a consequence of the use of the click chemistry toolbox to yield graft copolymers in an efficient manner. In particular, various alkyne and alkene functional lactones were synthesized including glycolide and caprolactone (CL) derivatives.[21–28] Halogenated lactones were also used to yield, after derivatization, copolyesters bearing clickable moieties.[29–31] The use of copper-catalyzed azide–alkyne cycloaddition (CuAAC) or thiol–ene thermal radical addition for the coupling of PEG-azide or PEG-thiol functions led to polyester-*g*-PEG structures in an elegant and controlled manner. Like for the "grafting through", one drawback of this approach lies, however, in the difficulty of synthesizing functional lactones in good yields. To overcome this limitation an alternative "grafting to" approach was followed by Coudane's group with the use of anionic post-polymerization modification to graft carboxyl PEG at the α-position of the carbonyl of pristine PCL.[32,33] This one pot method was rapid and versatile, and the graft copolymer was easily prepared on the multigram scale from a commercially available PCL. Unfortunately, a low control of the grafting density, and as a consequence, on the self-assembly behavior, was obtained.

To overcome this limitation, we present a simple and straightforward strategy to yield original amphiphilic PCL-*g*-PEG copolymers with controlled amphiphilicity. Advantage is taken of (i) the scale-up friendly post-polymerization modification technique to easily prepare, in one step, poly(α-propargyl-ε-caprolactone-*co*-ε-caprolactone) (PCL-yne) and (ii) of the fast, efficient and metal-free photo thiol–yne chemistry to synthesize the graft copolymers by reaction with a thiolated PEG (PEG-SH). Additionally, we demonstrate that good control of the copolymer composition, *i.e.* grafting density, is easily achieved. This is illustrated by the synthesis of PCL-*g*-PEG with EG/CL ratios ranging from 0.1 to 1.3 using the same reaction, namely a photoradical thiol–yne reaction. The family of amphiphilic PCL-*g*-PEG is then used to prepare pegylated nanospheres or core–shell micelles depending on the copolymer composition. As a proof of concept for use in drug delivery applications, we finally demonstrate the capacity of the polymeric micelles to encapsulate and release curcumin, a sensitive and potent chemotherapeutic anticancer drug with poor water solubility.

Materials and methods

Materials

PCL ($M_n \approx 45$ kg mol^{-1}), propargyl bromide (80 wt% in toluene), lithium diisopropylamide (2 M in THF/heptane/ethylbenzene), 2,2-dimethoxy-2-phenylacetophenone (DMPA, >99%), benzyl mercaptan (BM, >99%), *p*-toluenesulfonic acid monohydrate (>98%), mercaptopropionic acid (>99%), curcumin, Tween 80 and Span 80 were purchased from Sigma-Aldrich (St-Quentin Fallavier, France). α-Methoxy,ω-hydroxyl poly(ethylene glycol) (MeO-PEG) was obtained from Acros Organic Belgium. L(+)-Ascorbic acid puriss was obtained from Riedel-de Haen. Phosphate buffered saline (PBS) 10× was purchased from Gibco. NH_4Cl (>99%) was obtained from Acros Organics (Noisy-le-Grand, France), technical grade $MgSO_4$ from Carlo Erba (Val de Reuil, France), and methanol (≥99.8%), dichloromethane (DCM, ≥99.9%) and anhydrous tetrahydrofuran (THF, ≥99.9%) from Sigma-Aldrich (St-Quentin Fallavier, France). THF was distilled on benzophenone/sodium until a deep blue color was obtained. Spectra/por® dialysis tubes (cut-off, 6–8 kDa or 3.5 kDa) were obtained from Spectrum Labs.

Characterizations

NMR spectroscopy. ^{1}H NMR spectra were recorded at room temperature using an AMX300 Bruker spectrometer operating at 300 MHz. Deuterated chloroform and deuterated dimethyl sulfoxide were used as solvents, and chemical shifts were expressed in ppm with respect to tetramethylsilane (TMS). Diffusion ordered spectroscopy (DOSY) experiments were performed with a Bruker Avance III spectrometer operating at 600 MHz, using deuterated dimethyl sulfoxide (DMSO) as the solvent.

Size exclusion chromatography (SEC) was performed with a Waters equipment fitted with a 60 cm long 5 μm mixed C PLgel column and a Waters 410 refractometric detector. The mobile phase was chloroform at 1 mL min^{-1} flow rate at 30 °C. Typically, the polymer (10 mg) was dissolved in chloroform (2 mL) and the resulting solution was filtered through a 0.45 μm Millipore filter before injection of 20 μL of filtered solution. The number average molecular weight (M_n) and the dispersity ($Đ$) of the polymers were expressed according to calibration using polystyrene standards.

Fluorescence measurements and CAC determination. The CAC of the copolymers was determined by fluorescence spectroscopy using pyrene as a hydrophobic fluorescent probe. Measurements were carried out on an RF 5302 Shimadzu spectrofluorometer (Japan) equipped with a xenon light source (UXL-150S, Ushio, Japan). Briefly, an aliquot of pyrene solution (6×10^{-6} M in acetone, 1 mL) was added to different vials, and the solvent was evaporated. Then, 10 mL of aqueous solutions of different concentrations were added to the vials. The final concentration of pyrene in each vial was 6×10^{-7} M. After overnight equilibration at room temperature, the fluorescence emission spectra of the solutions were recorded from 350 to 400 nm at an excitation wavelength of 340 nm. The emission and excitation slit widths were 5 nm and 3 nm, respectively. The emission fluorescence values I_{373} and I_{384}, at 373 and 384 nm respectively, were used for subsequent calculations. The CAC was determined from the intersection of linear

regression lines of the I_{384}/I_{373} ratio *versus* polymer concentration plots.

Light scattering measurements. Dynamic light scattering (DLS) was carried out with a Malvern Instrument Nano-ZS equipped with a He–Ne laser (λ = 632.8 nm). Polymer solutions at 1.0 mg mL^{-1} were filtered through a 0.45 μm PTFE microfilter before measurements. The correlation function was analyzed *via* the general purpose method (NNLS) to obtain the distribution of diffusion coefficients (D) of the solutes. The apparent equivalent hydrodynamic diameter (D_H) was determined from the cumulant method using the Stokes–Einstein equation. Mean radius values were obtained from triplicate runs. Standard deviations were evaluated from hydrodynamic radius distribution.

Transmission electron microscope (TEM) micrographs were obtained with a JEOL 1200 EXII (working voltage of 120 kV). A drop of polymer solution at 1 mg mL^{-1} was placed onto a carbon-supported copper grid for 5 min. The excess liquid was removed by capillarity with a filter paper. The mean particle size was determined by measuring the particle diameter with Image J software (Rasband, W.S., ImageJ, U.S. National Institutes of Health, Bethesda, Maryland, USA, http://imagej.nih.gov/ij/, 1997–2014).

UV spectrometry was performed on a Perkin-Elmer Precisely Lambda 35 spectrometer, with 1 cm optical path quartz cuvettes.

PCL propargylation (PCL-yne)

The anionic chemical post-modification of PCL was obtained according to our previous work.[34] Typically, PCL (0.053 mol of CL unit, 6 g) was dissolved in anhydrous THF (300 mL) in a four-necked reactor equipped with a mechanical stirrer and kept at −50 °C under an argon atmosphere. A solution of LDA (0.5 eq. per CL unit, 13.2 mL) was injected with a syringe through a septum and the mixture was kept at −50 °C under stirring for 30 min. After this activation step, propargyl bromide (0.5 eq. per CL unit, 2.8 mL) was added, the mixture was kept under stirring and raised to −30 °C. After 30 min, the reaction was stopped by the addition of a saturated solution of NH_4Cl (100 mL) and the pH was adjusted to 7 with 1 M HCl. The polymer was extracted with DCM (3 × 150 mL). The combined organic phases were washed three times with distilled water (3 × 150 mL), dried on anhydrous $MgSO_4$ and filtered. After partial solvent evaporation under reduced pressure, the polymer was recovered by precipitation in cold methanol and dried overnight under vacuum. The polymer was obtained with an average yield of 79%.

^{1}H NMR (300 MHz; $CDCl_3$): δ (ppm) = 4.0 (2H, CH_2–O), 3.4 (2H, CH_2–OH), 2.4–2.6 (1H, C(O)CH(CH$_2$–C≡CH) and 2H, CH_2–C≡CH), 2.3 (2H, C(O)CH_2), 2.0 (1H, C≡CH), 1.6 (4H, C(O)CH$_2$–CH_2–CH$_2$–CH_2–CH$_2$–O), 1.4 (2H, C(O)CH$_2$–CH$_2$–CH_2–CH$_2$–CH$_2$–O).

PEG thiolation (PEG-SH)

MeO-PEG was dissolved in dry toluene in a round bottom flask and distilled by azeotropic distillation 3 times, and then dissolved in freshly distilled toluene. Mercaptopropionic acid (1.3 eq.) and *para*-toluene sulfonic acid (0.25 eq.) were added. The reaction was performed using a Dean–Stark apparatus under reflux of the solvent for 3 days. The solvent was evaporated under vacuum to yield oil that was precipitated in cold diethyl ether. The obtained polymer was filtered and dried under vacuum.

^{1}H NMR (300 MHz; $CDCl_3$): δ (ppm) = 4.2 (2H, CH_2COO), 3.6 (4H, CH_2CH_2O), 3.4 (3H, OCH_3), 2.8 (2H, CH_2SH), 2.7 (2H, COOCH_2), 1.6 (1H, –SH).

Model coupling reaction with benzyl mercaptan

In a typical experiment, PCL-yne (50 mg; 7% alkyne groups with respect to CL units) was dissolved in THF (1.5 mL) in a Schlenk flask (Table S1,† entry 2). Benzyl mercaptan (70 μL; 20 eq.) and DMPA (3.8 mg; 0.5 eq.) were added. The flask was covered by aluminum foil and purged with nitrogen for 10 min before closing. The reaction medium was then irradiated with UV light for 2 hours at room temperature under constant stirring using a DYMAX BlueWaveTM 200 equipment (100 mW cm^{-2}). After completion, the mixture was concentrated under vacuum and the oil was precipitated in heptane, before filtration of the polymer and drying under vacuum.

^{1}H NMR (300 MHz; DMSO-d$_6$): δ (ppm) = 7.2 (5H, C$_6H_5$), 3.9 (2H, CH_2–O), 2.2 (2H, C(O)CH_2), 1.5 (4H, C(O)CH$_2$–CH_2–CH$_2$–CH_2–CH$_2$–O), 1.2 (2H, C(O)CH$_2$–CH$_2$–CH_2–CH$_2$–CH$_2$–O).

Synthesis of PCL-*g*-PEG

In a typical experiment, PCL-yne (0.2 g; 8% alkyne groups with respect to CL units) and PEG-SH (1.0 g; 10 eq. with respect to alkyne groups) were dissolved in THF (15 mL) in a Schlenk flask (Table 1, entry 3). In parallel, DMPA (36 mg; 1 eq.) was dissolved in THF (15 mL) in a Schlenk flask covered by aluminum foil. The 2 flasks were purged with nitrogen for 10 min before closing with septums. The PCL-yne/PEG-SH reaction medium was irradiated with UV light for 2 hours (100 mW cm^{-2}) while DMPA was introduced by successive additions with a syringe at fixed intervals over the reaction time. After completion, the mixture was concentrated under vacuum and dialyzed against THF using cellulose tubing (molecular weight cut-off, 6000–8000 g mol^{-1}) until no residual free PEG was detected in SEC analyses. PCL-*g*-PEG was finally recovered after THF removal under vacuum and drying.

^{1}H NMR (300 MHz; $CDCl_3$): δ (ppm) = PCL backbone 4.0 (2H, CH_2–O), 2.3 (2H, C(O)CH_2), 1.6 (4H, C(O)CH$_2$–CH_2–CH$_2$–CH_2–CH$_2$–O), 1.3 (2H, C(O)CH$_2$–CH$_2$–CH_2–CH$_2$–CH$_2$–O); PEG side chains 4.2 (2H, CH_2COO), 3.5 (4H, CH_2CH_2O), 3.3 (3H, OCH_3), 2.8 (2H, CH_2SCH$_2$), 2.6 (2H, COOCH_2).

Preparation of micelles and nanospheres

Preparation of nanospheres. PCL-*g*-PEG nanospheres were prepared by the nanoprecipitation method. Briefly, PCL-*g*-PEG$_{0.1}$ (200 mg, EG/CL = 0.1) and Span 80 (100 mg) were dissolved in acetone (50 mL). The organic solution was slowly poured in 100 mL aqueous phase containing 200 mg of Tween 80 and maintained under vigorous stirring (9500 rpm) using

Table 1 Thiol–yne coupling of PEG-SH on PCL-yne

Entry	Copolymer	PEG-SH (eq. per alkyne)	Photoinitiator (DMPA) eq. per alkyne	Addition	EG/CL	Thiol–yne efficiency (%)	M_n	($Đ$)
1	PCL-*g*-PEG$_{0.35}$	5	0.25	Multiple	0.35	14	16 000	2.2
2	PCL-*g*-PEG$_{0.65}$	5	0.5	Multiple	0.65	24	20 000	2.6
3	PCL-*g*-PEG$_{1.15}$	10	1	Multiple	1.15	45	20 000	1.8
4	PCL-*g*-PEG$_{1.10}$	10	5	Multiple	1.1	44	24 500	3.0
5	PCL-*g*-PEG$_{1.30}$	15	1	Multiple	1.3	47	18 000	1.8

an Ultra-Turrax stirrer. After 4 hours of stirring, acetone and part of the aqueous phase were evaporated under vacuum. The solution was further dialyzed against water (cut-off, 6000–8000 g mol^{-1}) to eliminate Tween 80 and Span 80. For cryoprotection, 20 mg of glucose were added to the solution prior to freeze-drying of the nanospheres.

Preparation of micelles. PCL-*g*-PEG micelles were prepared by the self-assembly method. Briefly, PCL-*g*-PEG$_{1.15}$ (10 mg, EG/CL = 1.15; Table 1, entry 3) was dissolved in acetone (10 mL), and then rapidly poured into water (10 mL). The slow evaporation of acetone under atmospheric pressure for 24 h followed by a rapid evaporation under vacuum allowed the formation of the micelles.

Preparation of curcumin loaded micelles (Cur/PCL-*g*-PEG). The curcumin-loaded micelles were prepared by the self-assembly method. In a typical experiment, curcumin (5 mg) and PCL-*g*-PEG$_{1.15}$ (35 mg, EG/CL = 1.15; Table 1, entry 3) were dissolved in acetone (2 mL) before water (5 mL) addition. The resulting mixture was vigorously stirred for 1 hour using an Ultra-Turrax stirrer (8000 rpm). The remaining acetone was then removed by evaporation under vacuum. The resulting solution was centrifuged for 10 min at 10 °C at 3600 rpm prior to filtration through a 0.45 μm filter to eliminate the unloaded precipitated curcumin.

Determination of drug loading and encapsulation efficiency

Drug loading (DL) and encapsulation efficiency (EE) were determined by UV/Vis spectrophotometry at 425 nm. Quantification was performed with respect to a calibration curve of curcumin in acetone/water (20 : 80). The DL content and EE were calculated based on the following formulae:

$$\text{DL}\ (\%) = 100 \times (M_C)/(M_P + M_C)$$

$$\text{EE}\ (\%) = 100 \times (M_C)/(M_{Ci})$$

with M_C = mass of curcumin in micelles, M_P = mass of copolymer and M_{Ci} = mass of curcumin initially added to prepare micelles.

In vitro drug release assay

The release of curcumin from PCL-*g*-PEG micelles was assessed in phosphate buffer saline (PBS, pH 7.4) containing 0.1% w/v Tween 80 and 0.6% w/v ascorbic acid at 37 °C under constant orbital shaking (100 rpm; Heidolph Unimax 1010). Tween is classically used to provide water-solubility to curcumin in such assays.[35–37] Ascorbic acid is a biomolecule naturally present in plasma, which is used to enhance the stability and avoid the degradation of the released curcumin.[38] In a typical release study, 2 mL of Cur/PCL-*g*-PEG micellar solution were poured in a dialysis bag (cut-off 3.5 kDa) that was immersed in 20 mL of buffer solution at 37 °C. At specific time points, the entire release medium was removed and replaced with 20 mL fresh buffer solution. Collected samples were analyzed by UV-Vis spectrophotometry at 425 nm with reference to a calibration curve of curcumin in acetone : water (20 : 80). The amount of released curcumin (Rc) was calculated based on the following formula:

$$\text{Rc}\ (\%) = 100 \times (M_{RC})/(M_C)$$

with M_{RC} = mass of released curcumin and M_C = mass of curcumin in micelles.

Results and discussion

Synthesis of PCL-yne and PEG-SH

This work aims at developing a single chemical strategy to produce both micelles and nanospheres based on graft amphiphilic PCL-*g*-PEG copolymers. To this end, photoradical thiol–yne chemistry was chosen to graft PEG-SH to PCL-yne in a straightforward manner yet allowing control over the hydrophilicity/hydrophobicity balance. The strategy was chosen over the existing methods described in the literature and mentioned in the introduction part due to some important advantages: (i) time consuming and low yield synthesis of functional lactones is not required, (ii) PCL-yne can be prepared rapidly in high quantities, (iii) thiol–yne "click" grafting does not require metals, like copper, which is of benefit for medical use, and (iv) photo-chemical reactions are much faster than thermal thiol–ene or copper catalyzed reactions, thus preserving the integrity of the degradable polymeric chain.

In a first step, PCL bearing multiple alkyne groups (PCL-yne) was synthesized according to the anionic modification methodology recently reported by our group.[34] This method was chosen over copolymerization of α-propargyl-ε-caprolactone and ε-caprolactone as it allows one to easily obtain the functional PCL-yne on a multigram scale with substitution degrees of about 10 mol%. Optimized conditions defined in

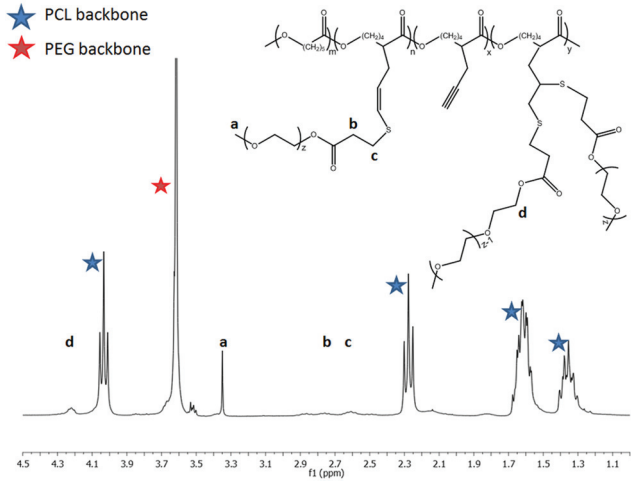

Fig. 1 ^{1}H NMR ($CDCl_3$, 300 MHz) spectrum of PCL-*g*-$PEG_{1.15}$.

our previous work were used. The polymer chemical structure was characterized by ^{1}H-NMR (ESI Fig. S1†). Typical signals of the propargyl group are found at 2.5 ppm, corresponding to the methylene proton, and at 2.0 ppm, corresponding to the alkyne proton. The substitution degree (SD) in the range 7–8% was calculated by comparison of the integrations of the resonance peak at 2.0 ppm with the integration of the resonance peak at 4.0 ppm, corresponding to a methylene of PCL. The molecular weight of PCL-yne was measured by SEC analysis in THF (Fig. 1). PCL-yne with molecular weight $\overline{Mn} = 21300$ g mol^{-1} and $Đ$ = 2.4 is obtained. These values were compared with the ones of the commercial PCL used as a starting material $\overline{Mn} = 40000$ g mol^{-1} and $Đ$ = 1.5. The molecular weight decrease is classically observed with the anionic activation of polyester, as a consequence of hydrolysis and backbiting side reactions.[39,40] In the present case, although remarkable in terms of influence on the final molecular weight, this corresponded to less than 0.3% hydrolysis of the ester groups initially present in the polymer chain. Noteworthily, starting from commercially available PCL, 5 g of PCL-yne was prepared on a single day, including reaction and purification thanks to this one pot and time saving reaction.

In a second step, PEG-SH was synthesized by esterification of the hydroxyl chain-end of MeO-PEG-OH by mercaptopropionic acid under classic conditions using a Dean–Stark continuous water distillation in toluene with *p*-toluene sulfonic acid as a catalyst. The extent of esterification was determined by ^{1}H NMR by comparison of the integration of the resonance peak at 4.2 ppm corresponding to the terminal methylene group of PEG in the α position of the ester group, with the integration of the resonance peak at 3.3 ppm, corresponding to the methylene groups of the PEG chain (ESI Fig. S2†). The esterification extent is found to be superior to 95%. PEG-SH was further characterized by SEC analysis in THF. A molecular weight of $\overline{Mn} = 1050$ g mol^{-1} ($Đ$ = 1.1) was calculated, which is in good agreement with $\overline{Mn} = 780$ g mol^{-1} ($Đ$ = 1.1) for the starting MeO-PEG.

Model coupling reaction with benzyl mercaptan

Recent efforts dedicated to post-polymerization modification of aliphatic polyesters have mainly focused on CuAAc reactions, with for example functional and graft PLA and PCL copolymers recently reported by our group.[22,24,41] Photoradical thiol–ene or thiol–yne, on the other hand, has been much less studied with few examples of chain-end functionalization,[42–44] and one recent example of PLA surface functionalization by our group.[45] To the best of our knowledge, only one example of photoradical thiol–yne multiple functionalization of polyesters has been reported by Zhang *et al.*, who prepared amino-functional PLA analogues using alkyne *O*-carboxyanhydride derived from tyrosine.[46] In this regard, benzyl mercaptan (BM) was first chosen as a model compound to evaluate the possibility of grafting multiple thiol derivatives on the PCL-yne backbone *via* photoradical thiol–yne addition. Parameters were selected based on reported conditions in the literature.[42] In particular, a large excess of BM was initially used (20 eq. per alkyne group). PCL-yne with 7% of CL units substituted with propargyl groups ($\overline{Mn} = 21200$ g mol^{-1}, $Đ$ = 2.4) and DMPA (0.5 eq. per alkyne group) as the photoinitiator were used for all experiments. The conditions are listed in ESI, Table S1.† SD was calculated from ^{1}H NMR analyses by comparison of the integrations of the resonance peak at 7.2 ppm, corresponding to the aromatic protons of BM, with the integration of the resonance peaks at 2.2 and 1.2 ppm, corresponding to methylene protons of PCL. One should note that the higher possible BM/CL ratio is 14% if quantitative diaddition of BM on alkyne groups is achieved. Under the classic conditions (ESI Table S1,† entry 1), high efficiency of the grafting is achieved with 75% reaction yield (1.5 BM grafted per alkyne group) and a resulting PCL bearing 10.5 mol% of BM groups with respect to CL units.

With the final aim to reduce the number of PEG-SH equivalents used in the next step, the impact of BM equivalents decrease was then evaluated with 10 eq. and 5 eq. (ESI Table S1,† entries 2 and 3). A similar reaction yield was obtained with 10 eq. whereas a lower yield (65%) was obtained with 5 eq. In both cases, higher dispersities were calculated with even a limited increase of molecular weight when 5 eq. BM were used. Our belief is that when low thiol equivalents are used, and taking into account that DMPA is already present in the mixture, part of the radicals that are generated under UV lead to a low extent of crosslinking side reactions instead of thiol–yne addition.

For this reason, further experiments were conducted with 10 eq., but with other parameters such as the use of quartz cuvettes and successive additions of the DMPA over the reaction time. Under these conditions, the final SD was unchanged (ESI Table S1,† entries 4–6) but successive additions of DMPA effectively reduced the impact on final dispersity. Molecular weights $\overline{Mn}$ in the range 15 000 g mol^{-1} to 22 000 g mol^{-1} and dispersity $Đ$ in the range 2.0–2.8 were obtained for all conditions except those for the entry 2 carried out in a quartz cuvette. In this case, a similar molecular weight is obtained

($\overline{Mn}$ = 19 000 g mol^{-1}) but with a very large distribution ($Đ$ = 5.1) and bimodality. This result is believed to be due to the strong impact of UV-B which are not filtered by a quartz vessel and may lead to both crosslinking and degradation of PCL-yne. For this reason a quartz vessel was not used in the rest of this study.

Although a quantitative BM thiol–yne coupling could not be reached, the extent of functionalization was high enough to further consider this approach for the synthesis of PCL-*g*-PEG. At this point one should note that, when considering polymer backbone functionalization, an important advantage of the thiol–yne reaction over the thiol–ene reaction is the ability for an yne-bond to react with two equivalents of thiol and to form a double addition product. This should clearly be of advantage to compensate for the expected lower reaction efficiency with a sterically hindered PEG-SH compared to BM.

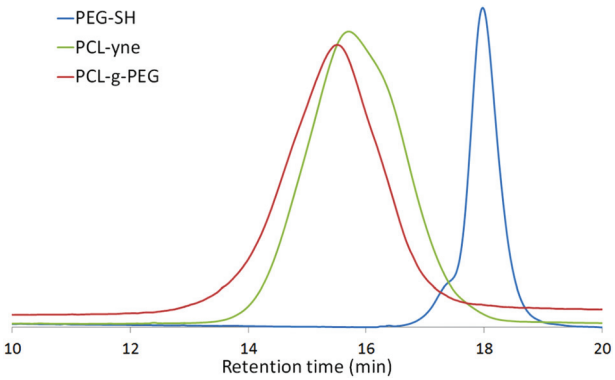

Fig. 2 SEC traces of PEG-SH (blue line), PCL-yne (green line) and PCL-*g*-PEG$_{1.15}$ (red line).

Synthesis of PCL-*g*-PEG

Although model coupling only focused on conditions aiming at a maximal grafting of BM, we were interested in evaluating the opportunities offered by the photoradical thiol–yne addition to generate a family of PCL-*g*-PEG amphiphilic copolymers with controlled hydrophilic/hydrophobic ratio. To this end, a parameter study was carried out by varying the number of PEG-SH and DMPA equivalents with respect to alkyne groups. These experiments are summarized in Table 1. Copolymers were analyzed by SEC and DOSY NMR to make sure that no free PEG-SH was remaining before ^{1}H NMR analysis to evaluate the grafting efficiency and the EG/CL ratio. As an illustration, the PCL-*g*-PEG$_{1.15}$ ^{1}H NMR spectrum is provided. The ^{1}H NMR spectrum exhibits signals corresponding to the PCL block (δ = 4.0 ppm, 2.3 ppm *etc.*; Fig. 1, blue stars) and to the PEG branches (δ = 3.5 ppm; Fig. 1, red star). As shown in the DOSY pattern (ESI Fig. S3†), ^{1}H NMR signals of the polyester backbone and PEG branches present the same diffusion coefficient consistent with efficient grafting of PEG-SH on the PCL-yne backbone. Moreover, no residual PEG-SH was observed as confirmed by the DOSY spectrum and the SEC trace of PCL-*g*-PEG copolymers (Fig. 2).

Considering the results obtained with BM, multiple additions of DMPA were done along the reaction time to avoid side reactions (*i.e.*, dimerization of PEG-SH or alkyne curing) and increase the addition efficiency. Under these conditions, increasing the number of DMPA equivalents from 0.25 up to 0.5 showed a beneficial effect on the grafting efficiency (entry 1 *vs.* entry 2). However, above 1 eq. DMPA a further increase was detrimental without an impact on the EG/CL ratio but with an increase of the dispersity that may be due to side reactions (*i.e.* crosslinking) occurring when high levels of radicals are present in the medium (entry 3 *vs.* entry 4). In a similar way, it was observed that although an increase of PEG-SH equivalents was beneficial, a limit was reached around 10 eq. as no drastic improvement of the EG/CL ratio was obtained at 15 eq. (entry 3 *vs.* entry 5).

Molecular weights measured by SEC were in the range of 16 000 g mol^{-1} to 25 000 g mol^{-1} with no significant changes in dispersities ($Đ$ = 1.8–2.6) except for the aforementioned entry 4 using 5 eq. of DMPA. Further discussion on the molecular weights of the copolymers with respect to PCL-yne ($\overline{Mn}$ = 21 200 g mol^{-1}, $Đ$ = 2.4) or comparison between the copolymers is not provided as the hydrodynamic behavior of the copolymers is known to be strongly impacted by their amphiphilicity and architectures. In particular, underestimation in the molecular weight of graft copolymers was reported in the literature and is believed to be due to the impact of grafting density on the hydrodynamic radius, which gives these graft copolymers more compact structures than their linear counterparts.[25,27] A typical SEC trace of the copolymer PCL-*g*-PEG$_{1.15}$ is however provided in Fig. 2 for illustration. In this case, a slight shift toward higher molecular weight is visible for the graft copolymer in comparison with the starting PCL-yne. More interesting is the efficiency of the coupling reaction. Starting with a PCL-yne with SD = 8%, the higher reachable EG/CL ratio with a theoretical PEG molecular weight of $\overline{Mn}$ = 750 g mol^{-1} is 2.6, which corresponds to 16% SD of a quantitative diaddition of thiol groups on alkyne groups. With a maximum of 1.3 the thiol–yne addition yield is *ca.* 50%. Not surprisingly this is lower than the 75% obtained with BM, but the grafting efficiency remained high when considering the disfavored grafting of multiple sterically hindered PEG-SH chains on a PCL-yne backbone. The determination of the extent of single hydrothiolation (monoaddition) and double hydrothiolation (diaddition) products was assessed by NMR analyses. No peaks corresponding to vinyl sulfide double bonds due to monoaddition and expected in the area 5.5–6.0 ppm could be found in the ^{1}H NMR spectra. Two explanations can be proposed. The first hypothesis is that only diaddition occurred in our system, which is in agreement with the previous studies of Fairbanks *et al.*, who observed that subsequent addition of a thiol to the vinyl sulfide intermediate is significantly faster (*ca.* 3 times faster) than the initial addition of a thiol to the alkyne.[47] Considering the strong steric hindrance generated by the successive PEG-SH additions, one can expect that only the more reactive site – vinyl sulfide – will react. Another more trivial explanation is that the extent of

vinyl sulfide present on the polymer might be too low for an accurate quantification under the experimental conditions.

To summarize, controlling the various parameters discussed above, it was possible to synthesize a family of amphiphilic PCL-*g*-PEG copolymers with a good control over the EG/CL ratios.

Self-assembly behavior of amphiphilic graft copolymers

The hydrophilic/hydrophobic balance has a significant effect on the self-assemblies that can be obtained. Being able to control the EG/CL ratio by thiol–yne coupling, we therefore used PCL-*g*-PEG copolymers to form various nanoaggregates. As an illustration, we chose to use a hydrophilic PCL-*g*-$PEG_{1.15}$ (Table 1, entry 3) to form micelles and to prepare an additional more hydrophobic PCL-*g*-PEG with EG/CL = 0.10 to generate nanospheres.

PCL-*g*-$PEG_{0.10}$ ($\overline{Mn}$ = 24 200 g mol^{-1}, $Đ$ = 1.9) was synthesized using 2 eq. of PEG-SH and a single addition of DMPA (0.5 eq.), all other conditions being the same as the ones previously used. Nanospheres were prepared by the nanoprecipitation method. PCL-*g*-$PEG_{0.10}$ might be seen as a block or a single branched copolymer as the EG/CL ratio of 0.1 roughly corresponds to one PEG_{750} side chain per PCL backbone. The nanospheres obtained were characterized by DLS and the hydrodynamic diameter D_H = 55 nm was found with PDI = 0.32 (Fig. 3).

Besides nanospheres, micelles were prepared from the copolymer PCL-*g*-$PEG_{1.15}$ that might be seen as a PCL backbone grafted with an average of 10 PEG_{750} segments. With a EG/CL ratio = 1.15 the direct dissolution method could not be used to induce self-assembly of the copolymers into micellar aggregates. Co-dissolution in a acetone/water mixture followed by acetone removal was used to produce the polymer micelles.

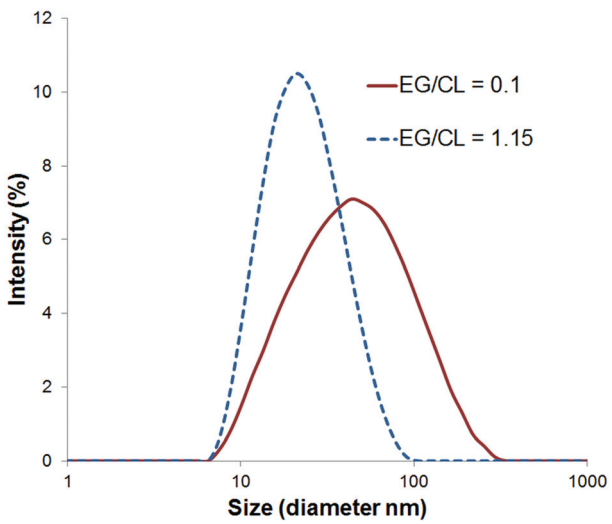

Fig. 3 DLS spectra of self-assembling nanospheres obtained from PCL-*g*-$PEG_{0.10}$ (plain line) and micelles obtained from PCL-*g*-$PEG_{1.15}$ (dashed line).

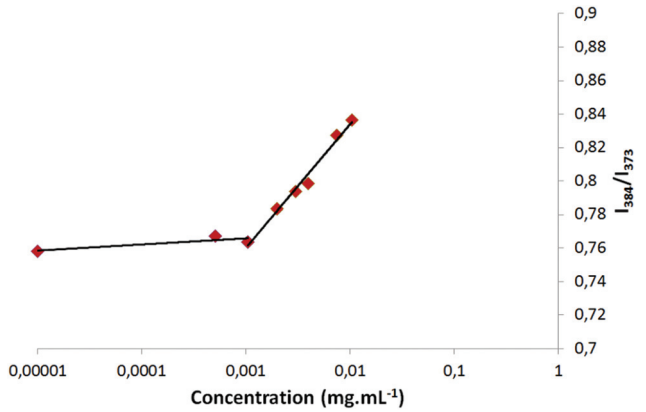

Fig. 4 Plot of the intensity ratios (I_{384}/I_{373} from pyrene emission spectra) as a function of concentration for self-assembling micelles in aqueous media from PCL-*g*-$PEG_{1.15}$.

The formation of micellar aggregates was first investigated by measuring the critical aggregation concentration (CAC) using fluorescence spectroscopy. Fluorimetry was achieved in emission with an excitation wavelength at λ_{ex} = 340 nm using pyrene as a fluorescent probe. The intensities of emission peaks at λ_{em} = 373 and 384 nm, denoted I_{373} and I_{384} respectively, were chosen as they are related to the polarity of the microenvironment in which pyrene was dissolved. Pyrene will preferentially partition into hydrophobic microdomains with a concurrent change in the molecule's photophysical properties. In the emission spectra a sharp rise in the intensity ratio of peaks at 373 and 384 nm of pyrene indicates the onset of aggregation (CAC) of copolymers (ESI, Fig. S4†). Fig. 4 shows the plot of the I_{384}/I_{373} intensity ratio against the copolymer concentration that was used for CAC calculation. The CAC value was determined from the intersection of the best-fit lines, which corresponded to the minimum polymer concentration required for the formation of aggregates in the aqueous medium. The CAC value of the PCL-*g*-$PEG_{1.15}$ copolymer was found equal to 1 mg L^{-1} (*ca.* 4 × 10^{-8} M) confirming the stability of the self-assembled micelles in aqueous solution. It is generally recognized that graft copolymers have low CMC because of the side chains reducing their mobility. Additionally, the relatively high dispersity of our copolymers ($Đ$ = 1.8) might also explain this low CAC as it has been demonstrated that for block copolymers the CMC is dependent on the dispersity, with lower CMC for higher $Đ$.[16]

The size distribution of micelles in water was determined by DLS. Fig. 3 shows the monodisperse distribution of the hydrodynamic diameter of the micelles with a mean hydrodynamic diameter D_H = 32 nm and PDI = 0.24. These values are in good agreement with previous studies on PCL-*g*-PEG copolymers. For example Zhang *et al.* reported on PCL_{10k}-*g*-PEG_{1k} copolymers ($\overline{Mn}$ = 10 100 g mol^{-1}, $Đ$ = 1.6) with a similar EG/CL ratio = 1.1 that formed micellar aggregates with D_H = 40 nm and PDI = 0.28 above a CAC = 1.8 mg L^{-1}.[31] For comparison, PCL-*b*-PEG-*b*-PCL triblock copolymers with a close EOG/CL

ratio = 0.94 had D_H = 47 nm with higher CAC = 11 mg L^{-1} whereas the PCL-*b*-PEG diblock copolymer with EG/CL = 1.2 had a reported CAC of 1×10^{-7} M (*ca.* 1.3 mg L^{-1}).[48]

This confirms that the self-assembly behavior of the PCL-PEG copolymer is influenced not only by the hydrophobic–hydrophilic weight fraction but also by the macromolecular architecture.[49] Architecture influences not only the CAC, but also the morphology of the aggregates. For example, it has been shown in the literature that PCL-*b*-PEG diblock copolymers with a low hydrophilic weight fraction prefer to form complex morphologies such as vesicle, cylindrical, and worm-like. PCL-*b*-PEG diblock copolymers with a PEG weight fraction of 30% (*i.e.* the same as the one calculated for our PCL-*g*-$PEG_{1.15}$) were reported to form short cylindrical micelles,[50] whereas spherical micelles are obtained with the PCL-*g*-PEG graft copolymers of the present work and that of Zhang *et al.*[31]

Finally, destabilization of the formed micellar aggregates was evaluated upon dilution of a micellar solution below CAC. In that case, no disappearance of micelles was observed which tends to demonstrate that the self-assemblies are not dynamic and that so-called frozen micelles have been formed. This is in agreement with the literature where it has been reported that, in opposition to small surfactants, the aggregates formed by copolymers are often not dynamic. The absence of copolymer chain exchange between the aggregates is responsible for this frozen state. In our case, this frozen state can be due to the crystallinity of the PCL core that physically blocks the copolymer chains in the aggregates. The frozen state can also be due to a very slow rate of exchange (kinetically frozen aggregates) that can be slowed down by the length of the hydrophobic PCL core, or the graft architecture.[51]

Curcumin loaded PCL-*g*-PEG micelles

The development of suitable drug delivery systems for insoluble drugs represents a major focus for pharmaceutical research and nanotechnology. Besides improved solubility, drug delivery systems can provide protection to the drug and thus increase its stability, while decreasing its associated side-effects. Micelles formed by PCL-*g*-$PEG_{1.15}$ have therefore been evaluated for drug encapsulation of an unstable drug, namely curcumin. Curcumin is extracted from the plant *Curcuma longa* and has demonstrated many pharmacological activities such as antioxidant, anti-inflammatory, chemo-preventive and anti-proliferative activities against a variety of cancers. However, the major disadvantages of curcumin are its low bioavailability, due to its poor aqueous solubility (11 ng ml^{-1}), and its poor stability.[38,52] Curcumin loaded micelles were prepared like blank micelles. The only difference was that curcumin was co-dissolved in acetone with the copolymer. Process parameters were optimized to increase the drug loading (DL) and encapsulation efficiency (EE). In that frame, the curcumin/copolymer ratios and the stirring rates were investigated (Table 2).

Magnetic stirring was less efficient to load micelles (low EE = 11 wt% and DL = 4.8 wt%). These values were greatly enhanced by stirring with Ultra-Turrax (EE = 55 wt% and DL = 10.2 wt%). This is clearly visible in Fig. 5b and c with a stronger yellow color obtained in the latter case compared to magnetic stirring. It is also important to note that in the absence of copolymer curcumin was totally insoluble as shown in Fig. 5a where precipitated curcumin is visible at the bottom of the test tube while no coloration of the solution appeared. Final improvement was obtained by changing the initial curcumin/copolymer ratio from 1 : 5 to 1 : 7. Under these conditions, near quantitative encapsulation was obtained (EE = 92 wt% and DL = 12.1 wt%). The influence of drug loading on the micelle size was evaluated by DLS analysis. Encapsulation of curcumin in the core of the micelles led to a small size increase from D_H = 32 nm for the blank micelles to D_H = 40 nm for the loaded micelles. TEM pictures (ESI, Fig. S5†) confirmed the spherical shape of the curcumin-loaded micelles. For comparison, data of the literature with diblock or triblock PCL/PEG copolymers with the same EG/CL ratio are provided in the ESI Table S2.† The results confirm the superiority of the graft copolymer compared to the block copolymers that led to limited EE = 77 wt% and DL = 9.6 wt% (ESI Table S2†). In all cases EE and DL are lower than in our graft copolymers with EE and DL in the order PCL-*g*-PEG > PCL-*b*-PEG-*b*-PCL > PCL-*b*-PEG. The compaction of the resulting self-

Table 2 Encapsulation efficiency and drug loading for curcumin loaded PCL-*g*-PEG_{15} micelles as a function of curcumin/polymer ratio and stirring

Entry	Type of copolymer	Curcumin/polymer (g : g)	Stirring conditions (rpm)	EE (wt%)	DL (wt%)
1	PCL-*g*-$PEG_{1.15}$	1 : 5	Magnetic (1000 rpm)	11	4.8
2	PCL-*g*-$PEG_{1.15}$	1 : 5	Ultra-Turrax (8000 rpm)	55	10.2
3	PCL-*g*-$PEG_{1.15}$	1 : 7	Ultra-Turrax (8000 rpm)	92	12.1

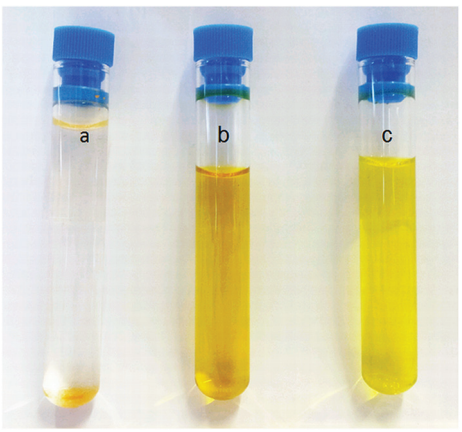

Fig. 5 Visual aspect of curcumin solutions without copolymer (a) , (b) within PCL-*g*-$PEG_{1.15}$ micelles using Ultra-Turrax stirring (Table 2 entry 2) or (c) within PCL-*g*-$PEG_{1.15}$ micelles using magnetic stirring (Table 2 entry 1).

assemblies is probably responsible for this result with an expected more compact PCL core with graft copolymers compared to the di- and triblock copolymer counterparts.

Finally, *in vitro* curcumin release was evaluated in PBS (pH = 7.4) at 37 °C. As classically described in the literature, low amounts of Tween 80 (0.1% w/v) were used to allow the solubilization of the released curcumin in PBS. In a first assay (data not shown), only 18% of curcumin were released after 16 days and no further release was then detected by UV-VIS analysis. This was due to the degradation of curcumin. As a consequence of its poor stability, once released from the micelles, curcumin was indeed rapidly degraded in the release medium, thus making analysis impossible for the longer time points. To overcome this limitation, various solutions have been proposed in the literature including pH lowering, or the addition of glutathione, *N*-acetyl-L-cysteine or ascorbic acid.[38] This last option was retained and ascorbic acid was added to the release medium at a concentration of 0.6 wt%.

Under these conditions, the stability of curcumin in the release medium was dramatically improved, thus allowing detection of the released drug over the all assay. Typical UV-visible absorption spectra recorded during the release study are provided in the ESI, Fig. S6,† and typical release profile is shown in Fig. 6. Curcumin release from the PCL-*b*-$PEG_{1.1}$ micelles was very slow over an 80 days period of time and without burst effect. Noteworthy is the almost complete release with up to 90% of initial curcumin being released, which proves that curcumin was efficiently protected from degradation in the micelles. This is remarkable as most studies related to curcumin encapsulation report on much faster kinetics and by far incomplete releases. Typically reported curcumin releases show a plateau at *ca.* 60% which is reached within 1 day to 12 days.[35–37,53] We believe that this difference can be ascribed to the graft architecture of our copolymer that yields frozen micelles with a more compact and probably crystallized PCL core. The higher molecular weight of the copolymer compared to the reported systems might also be responsible for this behavior. As a result the release obtained with the PCL-*g*-$PEG_{1.15}$ frozen micelles is more similar to the one expected with PCL nanospheres.

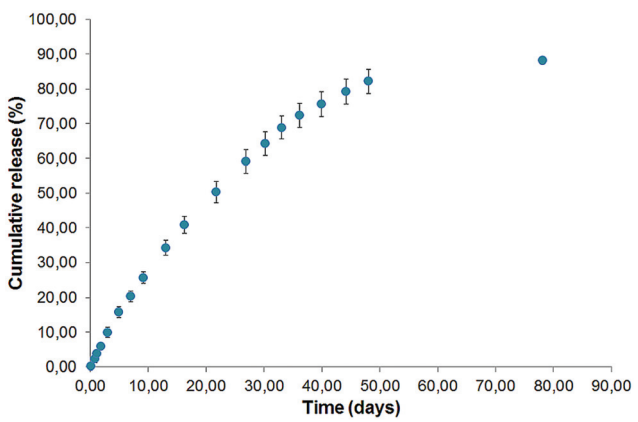

Fig. 6 Cumulative curcumin release from PCL-*g*-$PEG_{1.15}$ micelles (PBS, pH = 7.4, Tween 80 0.1% w/v; ascorbic acid 0.6 wt%). Data are expressed as means ± SD and correspond to measurements in triplicate.

Conclusion

A straightforward method for the synthesis of PCL-*g*-PEG copolymers has been reported. Using a combination of post-polymerization anionic chemical modification of PCL and thiol–yne photochemistry, a family of copolymers with controlled EG/CL ratios ranging from 0.1 to 1.3 was prepared. The chosen thiol–yne coupling approach, although suffering from a yield limited to 50% for the sterically hindered PEG_{750}, presents many advantages that make it a tool of choice for post-polymerization modification of PCL. Indeed, thiol–yne "click" grafting allows control of the composition, does not require metals, which is of benefit for medical use, and is fast compared to thermal reactions, which is beneficial to preserve the integrity of the degradable polymeric chains. Advantageously, this simple approach also offered opportunities for self-assemblies of nanospheres or micelles. The potential of PCL-*g*-PEG for drug encapsulation was demonstrated with curcumin. A slow but quasi-quantitative release was obtained, while efficient protection of the drug, higher encapsulation efficiency and higher drug loading than their linear counterparts were observed. We thus believe that the ease of PCL-*g*-PEG synthesis combined with the promising results shown with regard to drug delivery can offer opportunities in the field of encapsulation. Further studies of drug encapsulation and anticancer activity based on these novel PCL-*g*-PEG copolymers are underway and will be reported in due course.

Acknowledgements

The authors wish to thank the Azm & Saade Association for Assala Al Samad's fellowship, Stéphane Dejean for ^{1}H NMR analyses and Aurélien Lebrun of the Laboratoire de mesures physiques (LMP)-University Montpellier 2 for DOSY NMR analyses.

References

1 C. Timpe, *Am. Pharm. Rev.*, 2007, **3**, 104–109.
2 Y. Shi, W. Porter, T. Merdan and L. C. Li, *Expert Opin. Drug Delivery.*, 2009, **6**, 1261–1282.
3 Z. S. Ge and S. Y. Liu, *Chem. Soc. Rev.*, 2013, **42**, 7289–7325.
4 G. S. Kwon and K. Kataoka, *Adv. Drug Delivery Rev.*, 2012, **64**, 237–245.
5 H. Otsuka, Y. Nagasaki and K. Kataoka, *Adv. Drug Delivery Rev.*, 2012, **64**, 246–255.
6 Y. Wang and S. M. Grayson, *Adv. Drug Delivery Rev.*, 2012, **64**, 852–865.
7 K. Avgoustakis, *Curr. Drug Delivery*, 2004, **1**, 321–333.

8 G. Gaucher, R. H. Marchessault and J. C. Leroux, *J. Controlled Release*, 2010, **143**, 2–12.
9 J. Nicolas, S. Mura, D. Brambilla, N. Mackiewicz and P. Couvreur, *Chem. Soc. Rev.*, 2013, **42**, 1147–1235.
10 X. W. Wei, C. Y. Gong, M. Y. Gou, S. Z. Fu, Q. F. Guo, S. Shi, F. Luo, G. Guo, L. Y. Qiu and Z. Y. Qian, *Int. J. Pharm.*, 2009, **381**, 1–18.
11 R. Z. Xiao, Z. W. Zeng, G. L. Zhou, J. J. Wang, F. Z. Li and A. M. Wang, *Int. J. Nanomed.*, 2010, **5**, 1057–1065.
12 B. Nottelet, C. Di Tommaso, K. Mondon, R. Gurny and M. Moller, *J. Polym. Sci., Polym. Chem. Ed.*, 2010, **48**, 3244–3254.
13 B. Nottelet, M. Vert and J. Coudane, *Macromol. Rapid Commun.*, 2008, **29**, 743–750.
14 C. Hoskins, P. K. Thoo-Lin and W. P. Cheng, *Ther. Delivery*, 2012, **3**, 59–79.
15 J. Logie, S. C. Owen, C. K. McLaughlin and M. S. Shoichet, *Chem. Mater.*, 2014, **26**, 2847–2855.
16 Z. S. Gao and A. Eisenberg, *Macromolecules*, 1993, **26**, 7353–7360.
17 C. L. Lo, C. K. Huang, K. M. Lin and G. H. Hsiue, *Biomaterials*, 2007, **28**, 1225–1235.
18 X. W. Jiang, M. R. Smith and G. L. Baker, *Macromolecules*, 2008, **41**, 318–324.
19 J. Rieger, P. Dubois, R. Jerome and C. Jerome, *Langmuir*, 2006, **22**, 7471–7479.
20 R. J. Williams, R. K. O'Reilly and A. P. Dove, *Polym. Chem.*, 2012, **3**, 2156–2164.
21 D. E. Borchmann, N. ten Brummelhuis and M. Weck, *Macromolecules*, 2013, **46**, 4426–4431.
22 F. Coumes, V. Darcos, D. Domurado, S. M. Li and J. Coudane, *Polym. Chem.*, 2013, **4**, 3705–3713.
23 V. Darcos, S. Antoniacomi, C. Paniagua and J. Coudane, *Polym. Chem.*, 2012, **3**, 362–368.
24 S. El Habnouni, B. Nottelet, V. Darcos, B. Porsio, L. Lemaire, F. Franconi, X. Garric and J. Coudane, *Biomacromolecules*, 2013, **14**, 3626–3634.
25 X. Jiang, E. B. Vogel, M. R. Smith and G. L. Baker, *Macromolecules*, 2008, **41**, 1937–1944.
26 S. Onbulak, S. Tempelaar, R. J. Pounder, O. Gok, R. Sanyal, A. P. Dove and A. Sanyal, *Macromolecules*, 2012, **45**, 1715–1722.
27 B. Parrish, R. B. Breitenkamp and T. Emrick, *J. Am. Chem. Soc.*, 2005, **127**, 7404–7410.
28 Y. Yu, J. Zou, L. Yu, W. Jo, Y. K. Li, W. C. Law and C. Cheng, *Macromolecules*, 2011, **44**, 4793–4800.
29 H. Y. Li, R. Riva, R. Jerome and P. Lecomte, *Macromolecules*, 2007, **40**, 824–831.
30 R. Riva, P. Schmeits, F. Stoffelbach, C. Jerome, R. Jerome and P. Lecomte, *Chem. Commun.*, 2005, 5334–5336.
31 K. Zhang, Y. Wang, W. P. Zhu, X. D. Li and Z. Q. Shen, *J. Polym. Sci., Polym. Chem. Ed.*, 2012, **50**, 2045–2052.
32 J. Coudane, E. Laurent and M. Vert, *Macromol. Rapid Commun.*, 2004, **25**, 1865–1869.
33 S. Ponsart, J. Coudane, J. McGrath and M. Vert, *J. Bioact. Compat. Polym.*, 2002, **17**, 417–432.
34 A. Leroy, A. Al Samad, X. Garric, S. Hunger, D. Noel, J. Coudane and B. Nottelet, *RSC Adv.*, 2014, **4**, 32017–32023.
35 X. Gao, F. J. Zheng, G. Guo, X. X. Liu, R. R. Fan, Z. Y. Qian, N. Huang and Y. Q. Wei, *J. Mater. Chem. B*, 2013, **1**, 5778–5790.
36 L. Liu, L. Sun, Q. Wu, W. Guo, L. Li, Y. Chen, Y. Li, C. Y. Gong, Z. Qian and Y. Q. Wei, *Int. J. Pharm.*, 2013, **443**, 175–182.
37 H. Danafar, K. Rostamizadeh, S. Davaran and M. Hamidi, *Drug Dev. Ind. Pharm.*, 2014, **40**, 1411–1420.
38 Y. J. Wang, M. H. Pan, A. L. Cheng, L. I. Lin, Y. S. Ho, C. Y. Hsieh and J. K. Lin, *J. Pharm. Biomed. Anal.*, 1997, **15**, 1867–1876.
39 B. Nottelet, G. Tambutet, Y. Bakkour and J. Coudane, *Polym. Chem.*, 2012, **3**, 2956–2963.
40 S. Ponsart, J. Coudane and M. Vert, *Biomacromolecules*, 2000, **1**, 275–281.
41 V. Darcos, S. El Habnouni, B. Nottelet, A. El Ghzaoui and J. Coudane, *Polym. Chem.*, 2010, **1**, 280–282.
42 M. Bednarek, *React. Funct. Polym.*, 2013, **73**, 1130–1136.
43 T. Cai, M. Li, K. G. Neoh and E. T. Kang, *J. Mater. Chem.*, 2012, **22**, 16248–16258.
44 M. R. Molla and S. Ghosh, *Macromolecules*, 2012, **45**, 8561–8570.
45 C. Sardo, B. Nottelet, D. Triolo, G. Giammona, X. Garric, J. P. Lavigne, G. Cavallaro and J. Coudane, *Biomacromolecules*, 2014, **15**, 4351–4362.
46 Z. H. Zhang, L. C. Yin, Y. X. Xu, R. Tong, Y. B. Lu, J. Ren and J. J. Cheng, *Biomacromolecules*, 2012, **13**, 3456–3462.
47 B. D. Fairbanks, E. A. Sims, K. S. Anseth and C. N. Bowman, *Macromolecules*, 2010, **43**, 4113–4119.
48 (*a*) B. Xu, J. Yuan, T. Ding and Q. Gao, *Polym. Bull.*, 2010, **64**, 537–551; (*b*) D. Attwooda, C. Booth, S. Yeates, C. Chaibundit and N. Ricardo, *Int. J. Pharm.*, 2007, **345**, 35–41.
49 L. S. Zhang, J. P. Lin and S. L. Lin, *J. Phys. Chem. B*, 2007, **111**, 9209–9217.
50 Z. X. Du, J. T. Xu and Z. Q. Fan, *Macromol. Rapid Commun.*, 2008, **29**, 467–471.
51 T. Nicolai, O. Colombani and C. Chassenieux, *Soft Matter*, 2010, **6**, 3111–3118.
52 Z. M. Song, R. L. Feng, M. Sun, C. Y. Guo, Y. Gao, L. B. Li and G. X. Zhai, *J. Colloid Interface Sci.*, 2011, **354**, 116–123.
53 R. L. Feng, Z. M. Song and G. X. Zhai, *Int. J. Nanomed.*, 2012, **7**, 4089–4098.